Catalysis Today 159 (2011) 100–107

Contents lists available at ScienceDirect

Catalysis Today

journal homepage: www.elsevier.com/locate/cattod

Soot-catalyst contact studies in combustion processes using nano-scaled ceria as test material

Lars Hensgen, Klaus Stöwe*

Lehrstuhl für Technische Chemie Universität des Saarlandes, Campus C4.2, 66123 Saarbrücken, Germany

ARTICLE INFO

Article history:
Available online 27 April 2010

Keywords:
Particulate matter combustion
Lean conditions
Catalyst-soot contact

ABSTRACT

Combustion temperatures of particulate matter of Diesel automobile engines under lean conditions in laboratory experiments depend on a number of parameters: e.g. model gas composition and flow rate, catalyst composition and micro structure, soot/catalyst ratio as well as model soot type (composition, particle size and size distribution) and contact type. Especially the last two factors are often underestimated. In the literature most commonly Printex U and loose or tight contact are used. Here we report on the effect of these two parameters by varying the soot used and contact type and with nano-scaled ceria as catalyst due to its known Oxygen Storage Capacity (OSC). Apart from investigating the influence of these factors our second main objective was to find a preparation technique for the soot-catalyst contact, which fulfills the criteria of high reproducibility, high comparability to real conditions and facile automation. The last criterion is the basis for its use in high-throughput techniques (HTT) for parallelized discovery and optimization studies of new combustion catalysts.

1. Introduction

Quite early it was recognized that the addition of catalyst materials to soot has an effect on the combustion temperatures. Three major problems are related to this process: (1) the catalyst material itself, (2) the soot type used and (3) the contact between soot and the catalyst.

Since real soot collected from Diesel engines under real conditions has an irreproducible composition strongly dependent on engine parameters, model soots are used for these investigations, and in most reports Printex U carbon black (PU) from Evonik–Degussa is used. Since the topic of catalytic soot combustion is very intensely discussed in literature, we focus in this introduction on ceria as catalyst.

In 1996, Neeft et al. found that the intensity of contact between soot and catalyst is one of the major parameters that determine the soot oxidation rate (tight or loose contact) [1]. Various oxides have been tested in this study by TGA/DSC and heat flux maxima are given. Ceria was tested only in tight contact with 21% O_2 with a $T_{max} \approx 567\,^{\circ}C$ (taken from Fig. 3). Tight contact was also used in the thermogravimetric investigations by Lamonier et al. They prepared ceria and ceria-zirconia solid solutions by (co-)precipitation with ammonia and observed combustion of N330 soot with 20% O_2 in a 2-step process with a first maximum in DTG at about 340 °C [2].

Apart from combustion temperatures also often other parameters are evaluated as for instance the activation energy for the combustion process by Dernaika and Uner. In their study they used a self-made soot and observed by TGA with 20% O_2 values of T_5, T_{max}, T_{99} of 480, 570, and 650 °C, respectively, without specifying the soot-catalyst contact mode [3].

Bueno-Lopez et al. [4] and Setiabudi et al. [5] used a TAP (temporal analysis of products) reactor to study the mechanism of the soot combustion with and without the influence of NO_2 using labelled oxygen. Apart from lattice oxygen (OSC) of ceria, they propose the presence of surface superoxide species O_2^- generated from NO_2 as being responsible for the low combustion temperatures of this and similar compounds.

Instead of TGA/DTA/DSC investigations often the relative CO_2 concentration from TPO (temperature programmed oxidation) studies are reported that were measured for instance by gas chromatography (GC). Aneggi et al. give in several papers the results of studies with 6% O_2 in tight contact mode not specifying the soot type used. It is shown that ceria (also doped with transition metals (Zr and Fe) and rare earth elements (La, Pr, Sm, Tb)) results in active catalysts with enhanced textural properties and peak-top temperatures in tight-contact as low as $T_m = 387\,^{\circ}C$ [6–8].

The physico-chemical properties of ceria and rare earth modified ceria (with La, Pr, Sm, Y) catalysts are also studied and correlated with the soot oxidation activity with O_2 and $O_2 + NO$ by Krishna et al. [9] Their results based on TGA data with Printex U soot in tight and loose contact in 20% O_2 resulted in T_{50} values

* Corresponding author. Tel.: +49 681 302 64119.
E-mail address: k.stoewe@mx.uni-saarland.de (K. Stöwe).

0920-5861/$ – see front matter © 2010 Elsevier B.V. All rights reserved.
doi:10.1016/j.cattod.2010.03.070

not lower than 400 °C (no details given). Later they extended their investigations on other dopants [10–12].

Not precipitation or nitrate decomposition, but water in oil (W/O) emulsions were used by Mełecka et al. to produce nano-sized (4–5 nm) CeO_2 and $CeLnO_x$ mixed oxides with narrow size distribution. With PU soot in tight contact in 20% O_2 they get according to TGA results a T_{50} = 507 °C [13]. The high initial activity according to FT-IR measurements was due to the synergetic effect of nitrate groups present in the highly disordered surface of nano-crystalline Ln_2O_3, which enhanced the reductivity of nano-crystalline CeO_2. An example for the precipitation preparation method is the report of Atribak et al., who give a T_{50} = 575 °C for PU soot in loose contact in 5% O_2 [14]. Others use the solution combustion method (SCS) using urea for synthesis and observe in TPO measurements with a real Diesel soot (18.75% HC) in either loose or tight contact (not specified) with 20% O_2 a T_{max} = 405 °C [15,16].

A large step towards the understanding of the soot combustion process was given by Simonsen et al. [17]. From a time-lapsed environmental transmission electron microscopy (ETEM) image series of soot particles (Printex U) in contact with CeO_2, or with Al_2O_3 as an inert reference, mechanistic and kinetic insights into catalytic and non-catalytic oxidation mechanisms were obtained. The results indicated that the catalytic soot oxidation mechanism involves the reaction of centres at the soot-CeO_2 interface and that the interface reaction kinetic properties were in good agreement with previous macroscopic measurements.

With the soot MA7 of Mitsubishi Corp., tight contact mode and 20% O_2 Machida et al. observed from TGA data a light-off (ignition) temperature of T_i = 347 °C [18]. ESR measurements showed that the presence of O_2 in the gas phase is resulting in O_2^- ions at the surface of ceria. Such reactive oxygen species were less abundant on CeO_2–ZrO_2 and were not detected on ZrO_2 and Pr_6O_{11}. They emphasize that not only the OSC is a crucial parameter in soot combustion, but also the spill-over behaviour of the corresponding oxide.

Also high-throughput (HT) methods are in the process of being developed and used for the evaluation of Diesel soot oxidation catalysts. The optimal experimental conditions (soot amount, catalyst/soot ratio, type of contact, composition and flow rate of gas reactants) ensuring a reliable and reproducible detection of light-off temperatures in a 16 parallel channel reactor were evaluated. Using ceria HSA from Rhodia with a surface area of 325 m^2/g, real Diesel engine soot and a flow rate of 40 mL/min TPO measurements resulted in light-off (ignition) temperatures of T_i = 310 °C for tight and T_i = 370 °C for loose contact in 50% O_2 and T_i = 335 °C for tight contact in 10% O_2. From an HT screening of a large diverse library (over 100 mixed oxides catalysts) under optimized conditions, about 10 new formulations were found to perform better than commercial ceria and perovskite reference materials [19].

All in all we can summarize that the conditions to test for soot combustion are rather widespread: the oxygen content in the test gasses vary between 5% and 50%, the gas flow rates are commonly not specified, the gas composition may include promoting nitrogen oxides or not, as soot most commonly PU is used, but also other types, the contact is exclusively loose or tight, often even not specified, and type of data evaluation differs distinctively, ranging from initial temperatures T_i to maximum temperatures T_m determined by various methods ranging from thermoanalytical to gas chromatographical methods. In conclusion all these data are very difficult to compare.

2. Experimental procedures

As catalysts several VP AdNanoCeria 50 samples supplied by Evonik-Degussa with different particle sizes and BET-surfaces were used. In detail these were VP AdNanoCeria 50 with lot no. PH36703 and S_{BET} = 22 m^2/g, lot no. PH36701 and S_{BET} = 60 m^2/g, and lot no. PH36702 and S_{BET} = 90 m^2/g. These have been prepared by flame spray pyrolysis. As carbon source three different species of soot were used: fullerene soot (Aldrich) with >7% fullerenes, Printex U soot (Evonik–Degussa) and Printex 90 soot (Evonik–Degussa). They were used as supplied.

For all tested soot-catalyst contact modes the soot/catalyst ratio was fixed to 1:4. The loose contact was prepared by mixing manually 1 g CeO_2 and 250 mg of soot in a 20 ml snap–cap jar with a spatula for 1 min until a homogeneous mixture of ceria and soot was received. For the tight contact 1 g CeO_2 and 250 mg of soot was manually pestled in an agate mortar until a homogeneous mixture was obtained. To obtain pressure contact, about 100 mg of the loose contact mixture was pressed in a hydraulic press with 5 t load and the pellet formed was subsequently crushed to a powder in an agate mortar. The new wet contact was created by stirring 1 g CeO_2 and 250 mg of soot in 15 ml of organic solvent such as acetone with 350 rpm of a magnetic stirring bar for 6 h. Additionally the stirring time was varied within 30 min steps. At the beginning of the stirring period both, soot and ceria, tend to separate, but with stirring time these differences vanish and a uniform suspension forms. Consequently, the achieved contact is also depending on the stirring time, the distinct reproducibility of the wet contact being also due to fixed experimental conditions without any influences due to operating personnel as for tight and loose contact modes. Subsequently the solvent was removed by overnight drying at T = 40 °C in a laboratory-type drying cabinet.

The TGA/DSC-measurements were performed with an automated TGA analyzer MettlerToledo TGA/DSC1 with a 32-fold autosampler. The gas flow of 50 mL/min 8% oxygen in nitrogen was adjusted by mass flow controllers (MFC). Also the promoting effect of NO addition was tested, but is not reported here. The sample was heated from 25 to 700 °C with a heating rate of 2 °C/min. To characterize the soot combustion the T_{50} values of the thermogravimetric curves after buoyancy corrections were used. The T_{50} value is the temperature where 50% of the determined mass loss has occurred. As starting point for the mass loss a temperature of 150 °C was selected to exclude the mass loss of adsorbed water on the catalyst surface. The end point was 700 °C.

Nitrogen physisorption measurements were performed on a Carlo Erba Sorptomatic 1990 at a temperature of −196 °C. All samples were outgassed for 2 h under vacuum at 200 °C before adsorption. The powder X-ray diffraction (XRD) patterns were obtained with a Huber G670 Guinier camera with $CuK_{\alpha 1}$-radiation (λ = 1.54056 Å) and Rietveld refinements of the diffraction pattern were performed with the program TOPAS [20,21]. Because crystallite size is a quantity, which cannot be measured directly, so-called column heights are given. These are volume weighted averages and

Table 1
Soot type specifications and characterization data.

Soot type	Particle size by supplier	S_{BET} [m^2/g]	r_{max} [nm]*	r_{med} [nm]*	V_{pores} [cm^3/g]*
FS	>7% fullerene	241.7	1.32	6.49	0.1152
P90	ca. 15 nm	296.0	1.67	5.19	0.2681
PU	ca. 30 nm	109.9	1.51	4.62	0.1883

* Determined by BJH method.

are only identical with the crystallite size for *h* 0 0 reflections and cubic crystals. Any crystallite size term can only be used tentatively, to obtain the true crystallite size the true mean shape of the crystallites must be known. Here, a FWHM based measure for the crystallite size assuming purely Lorentzian-type crystallite size broadening is specified.

3. Results and discussion

3.1. Soot and catalyst characterization

In this preliminary investigation several fundamental problems should be addressed: which model soot and which artificial, laboratory-generated contact type is the most appropriate one for modelling the actual contact situation in soot combustion of real Diesel particle filters (DPF) and can be applied and studied by HT methods.

Diesel soot particulate matter consists of amorphous carbon, on which hydrocarbons (HC) are adsorbed, frequently termed as soluble organic fraction (SOF) including polycyclic aromatic hydrocarbons (PAH and nitro-PAH), but also sulfates, water and trace elements such as Zn, P, Ca, Fe Si, Cr. The exact particulate matter (PM) composition depends on engine operating parameters, such as load, number of revolutions, operating temperature. Especially the SOF fraction is strongly dependent on cylinder temperature. Therefore the collection of reproducible soot qualities is difficult or even impossible to realize. Thus, usually carbon blacks are used as model soot. These consist of pure elemental carbon and are dissimilar to soot in that sense that they have a significantly smaller PAH content (e.g. Printex U from Evonik–Degussa contains less than 0.3% HC extractable with toluene). Fino et al. showed that carbon blacks have higher combustion temperatures than amorphous carbon and both higher combustion temperatures than Diesel PM, so carbons blacks can be regarded as a pessimistic estimate for soot combustion temperatures [22]. HRTEM investigations of Diesel soot PM by Schlögl and co-workers revealed that also the particle size depends on operating conditions. An Euro 4 engine and a "black smoker", i.e. a D2876 CR engine at 30% load, artificially adjusted for high soot emission by air throttling and reducing rail pressure with blackening number 5, produced soot with average particle diameters of 13 and 35 nm, respectively. Additionally the soot collected with an Euro 4 engine showed in TEM images a high fraction of fullerene-like structures [23]. This observation together with the average particle sizes led us to select the following three model soot for the subsequent experiments: the FS soot because of its high fullerene content of more than 7%, the Printex 90 soot because of its particle size just in the range specified for an Euro 4 engine and the Printex U soot as reference. Table 1 gives BET measurement results of the three model soot. According to these data the sur-

Table 2
Powder XRD data and Rietveld refinement results of VP AdNanoCeria 50 with different BET surface areas.

VP AdNano Ceria 50 with nominal surface area [m^2/g]	Lattice parameter [Å]	Lorentzian-type crystallite size broadening L [nm]
22	5.4080(2)	68(1)
60	5.4116(3)	26.7(2)
90	5.4036(4)	19.1(2)

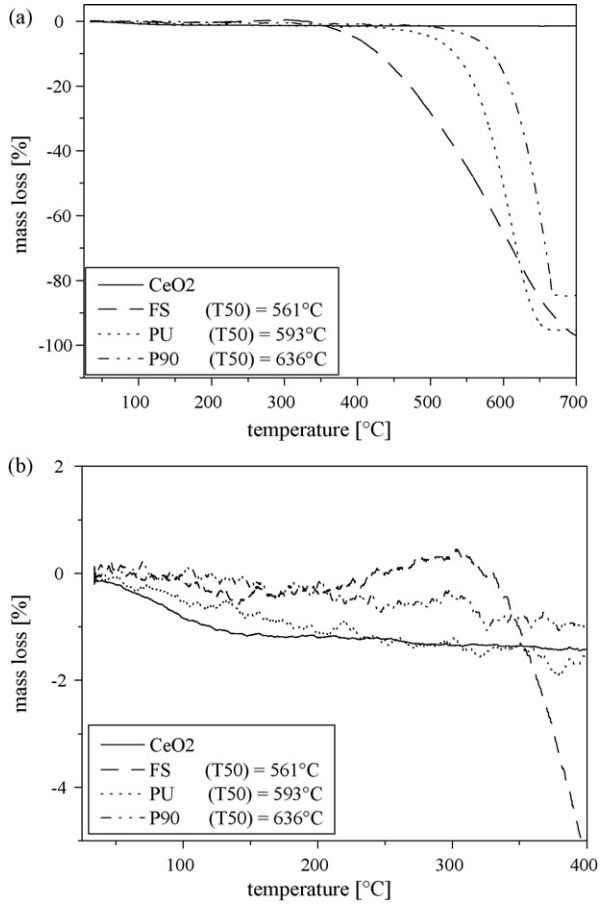

Fig. 1. Thermal weight loss of the starting materials a) full range curves b) detail of part a) (TGA-measurements 8% O_2 in N_2; 25–700 °C with 2 °C/min).

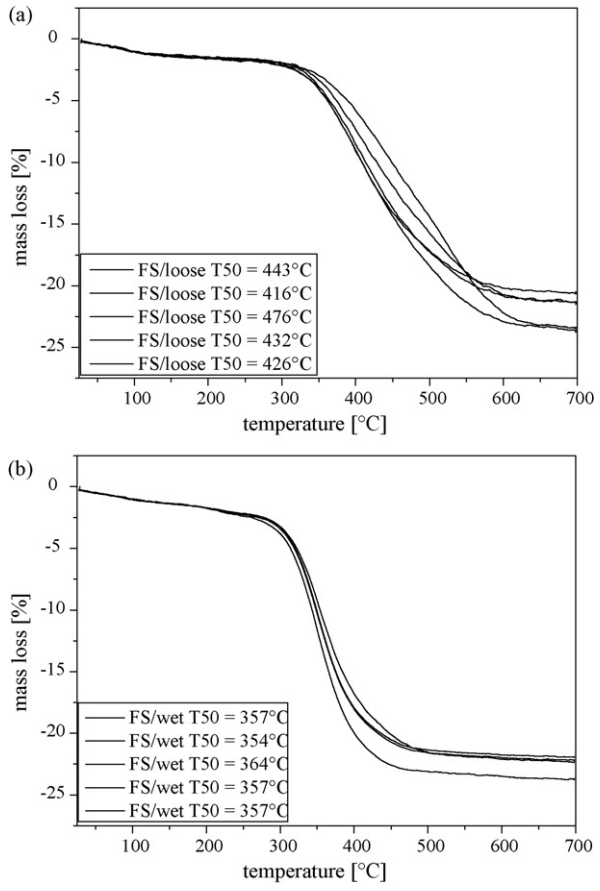

Fig. 2. Reproducibility measurements a) fullerene soot with loose contact; b) fullerene soot with wet contact (8% O_2 in N_2; 25–700 °C with 2 °C/min).

face area of the Printex U soot is the lowest one, lying just above S_{BET} = 100 m^2/g. The other two soot types have surface areas well above S_{BET} = 200 m^2/g (241.7 and 296.0 m^2/g) with the P90 soot revealing the smallest particles and accordingly the highest surface area.

The ceria supplied by Evonik–Degussa is not a commercial but a research product produced by flame spray pyrolysis with different surface areas: 22, 60 and 90 m^2/g. These data have been verified for one of these powders, revealing for VP AdNanoCeria 50 a surface area of 63 m^2/g. Additionally powder X-ray diffraction pattern have been accumulated resulting in data given in Table 2. As a measure for the crystallite size here Lorentzian-type crystallite size broadening from Rietveld refinements with TOPAS were specified. As expected, increasing surface area and decreasing crystallite size proceed parallel and at the highest surface area the crystallite size of the ceria and the particle size of the P90 soot (and probably also the FS soot) are comparable, so that an intimate mixture of the two can be expected. As TEM images revealed, the primary particles of the VP AdNanoCeria 50 are agglomerated to larger secondary aggregates (see Section 3.3).

The starting materials (fullerene soot, Printex U soot, Printex 90 soot and VP AdNanoCeria50 with S_{BET} = 60 m^2/g) have been analyzed with TGA/DSC, using a heating rate of 2 °C/min from 25 to 700 °C with 8% O_2 in N_2. This gas mixture was chosen because the oxygen level of 8% is a typical concentration in the exhaust of a common Diesel vehicle at full load [24,25]. Furthermore other gases are not used (such as NO, propane and CO), because they can have a reducing effect on the materials. Fig. 1a shows the thermal weight loss of the different soot types and the VP AdNanoCeria 50. Apart from desorption of water CeO_2 did not show any remarkable mass loss. The lowest T_{50} temperature of the three model soot had the FS soot with 561 °C, followed by the Printex U soot with 593 °C and at least the Printex 90 soot with 636 °C. In Fig. 1b the *y*-axis is spread and the region around the initial weight at the beginning of the measurement is depicted. It reveals that the fullerene soot after the desorption of water in contrast to the other soot types shows a mass increase, which is reproducible and which we associate with the inclusion of gas species within the fullerene molecules of this type of soot.

Table 3
Reproducibility and homogeneity of the different contacts.

Contact	Loose	Wet
T_{50}/rep. 1	443 °C	357 °C
T_{50}/rep. 2	416 °C	354 °C
T_{50}/rep. 3	476 °C	364 °C
T_{50}/rep. 4	432 °C	357 °C
T_{50}/rep. 5	426 °C	357 °C
Mean value	439 °C	358 °C
Standard deviation $\sigma(T_{50})$	23.1 °C	3.7 °C
Mass loss rep. 1	−21.3%	−21.9%
Mass loss rep. 2	−20.5%	−23.7%
Mass loss rep. 3	−23.5%	−22.3%
Mass loss rep. 4	−23.7%	−22.2%
Mass loss rep. 5	−21.4%	−22.2%
Mean value	−22.1%	−2.5%
Standard deviation $\sigma(T_{50})$	1.4%	0.7%

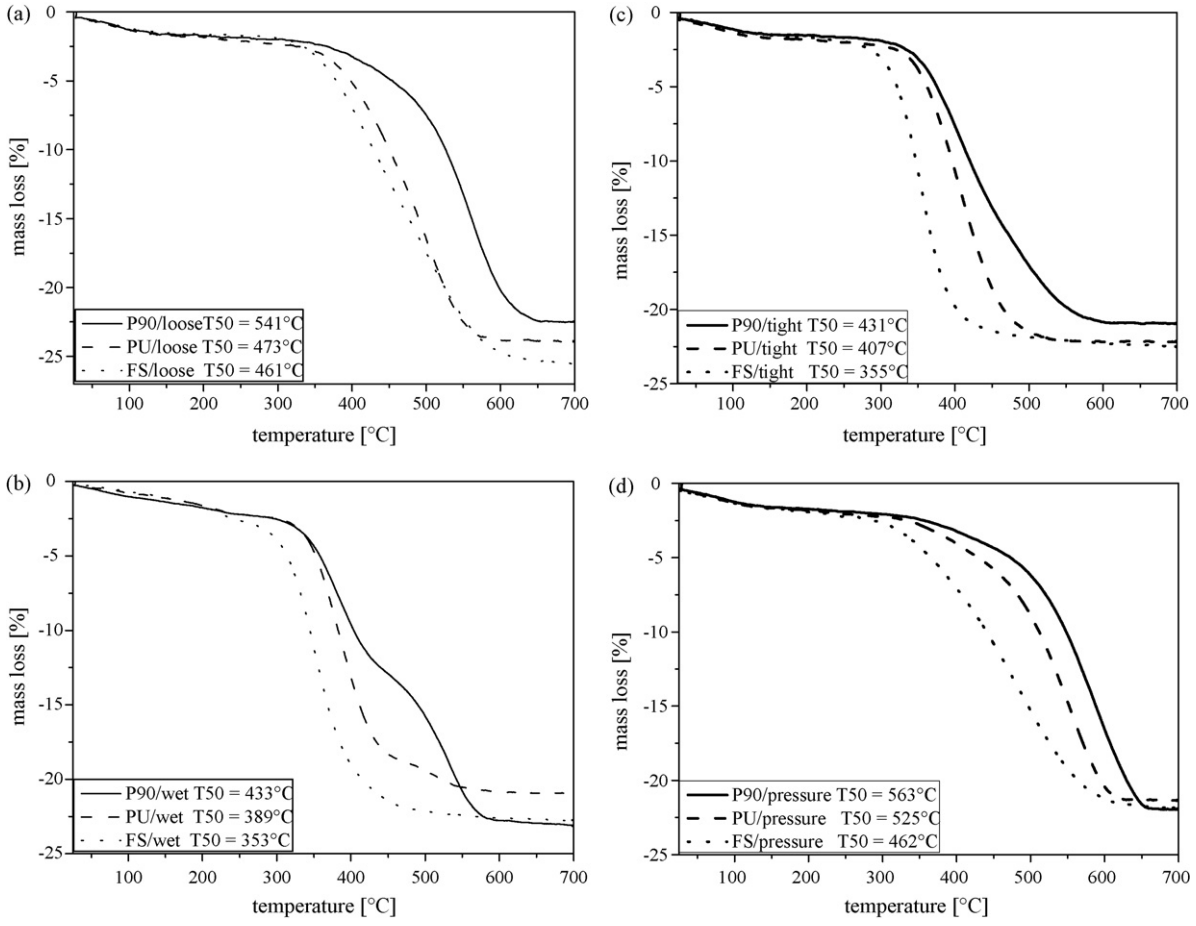

Fig. 3. Thermogravimetric measurement with the same contact and different soot types a) loose contact; b) wet contact; c) tight contact; d) pressure contact (8% O_2 in N_2; 25–700 °C with 2 °C/min).

3.2. Contact type evaluations

In the literature there are three contact modes known: loose [26], pressure [27] and tight contact [28]. To compare different catalysts in HT experiments it is very important, that a contact has a high reproducibility concerning the T_{50} values and a high homogeneity. The problem of the tight contact is that the T_{50} temperatures are much lower than in commercial DPF [22] and the parallelization of this contact is only possible in combination with very high costs. The T_{50} temperatures of the loose and the pressure contact are similar to the temperatures in the real DPF systems, but the problem of these contacts is that no automation is possible. In a typical HT workflow with iterations of a number of operations, as for instance synthesis and characterization, a manual step will be the rate determining one. To check the reproducibility and the homogeneity of the loose contact, five samples have been prepared by the same method and measured under identical conditions (see Fig. 2a). The T_{50} values and the percentaged buoyancy corrected mass loss have been compared (Table 3). With a standard deviation of $\sigma(T_{50}) = 23.1\,^{\circ}C$ the reproducibility of the loose contact is poor. To reach a better reproducibility a new contact mode had to be developed. This new contact was created by stirring the soot with the catalyst in acetone for 6 h. With this new wet contact a better reproducibility (Fig. 2b), with a $\sigma(T_{50})$ of only 3.7 °C could be reached. Also the homogeneity of the sample in the wet contact is better than in the loose contact (Table 3). Another advantage of the new wet contact is that it is more suitable for par-

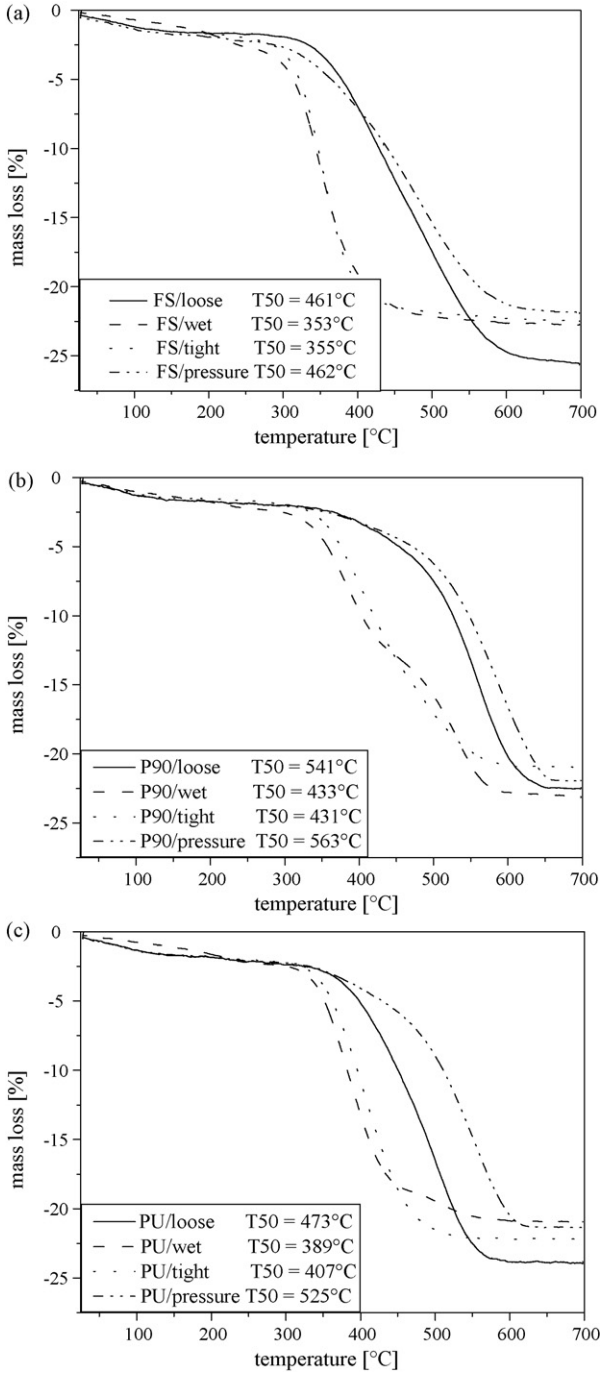

Fig. 4. Thermogravimetric measurement with one soot and different contacts a) fullerene soot contact; b) Printex U soot; c) Printex 90 soot (8% O_2 in N_2; 25–700 °C with 2 °C/min).

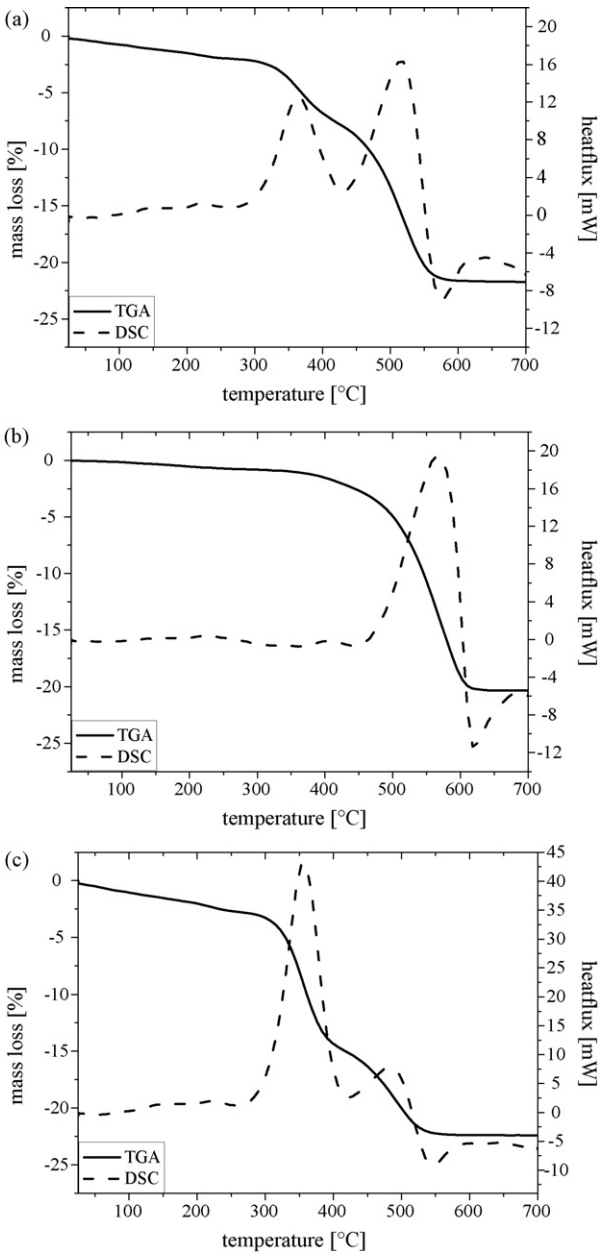

Fig. 5. Thermogravimetric and differential scanning calorimetric measurements of a wet contact mode mixture of P90 soot and ceria. a) VP AdNanoCeria 50 with $S_{BET} = 60\,m^2/g$; b) VP AdNanoCeria 50 with $S_{BET} = 22\,m^2/g$; c) VP AdNanoCeria 50 with $S_{BET} = 90\,m^2/g$ (8% O_2 in N_2; 25–700 °C with 2 °C/min).

allelization than the other classic (loose, tight and pressure) contact modes.

To check the influence of the soot types on the contact mode, the three different types of soot (fullerene soot (FS), Printex U (PU) and Printex 90 (P90)) were measured in combination with the four different contact modes. In each contact mode (loose, tight, wet and pressure) the T_{50} values of the FS were lower than those for the PU and the P90 soot. Note that the P90 soot had always the high-

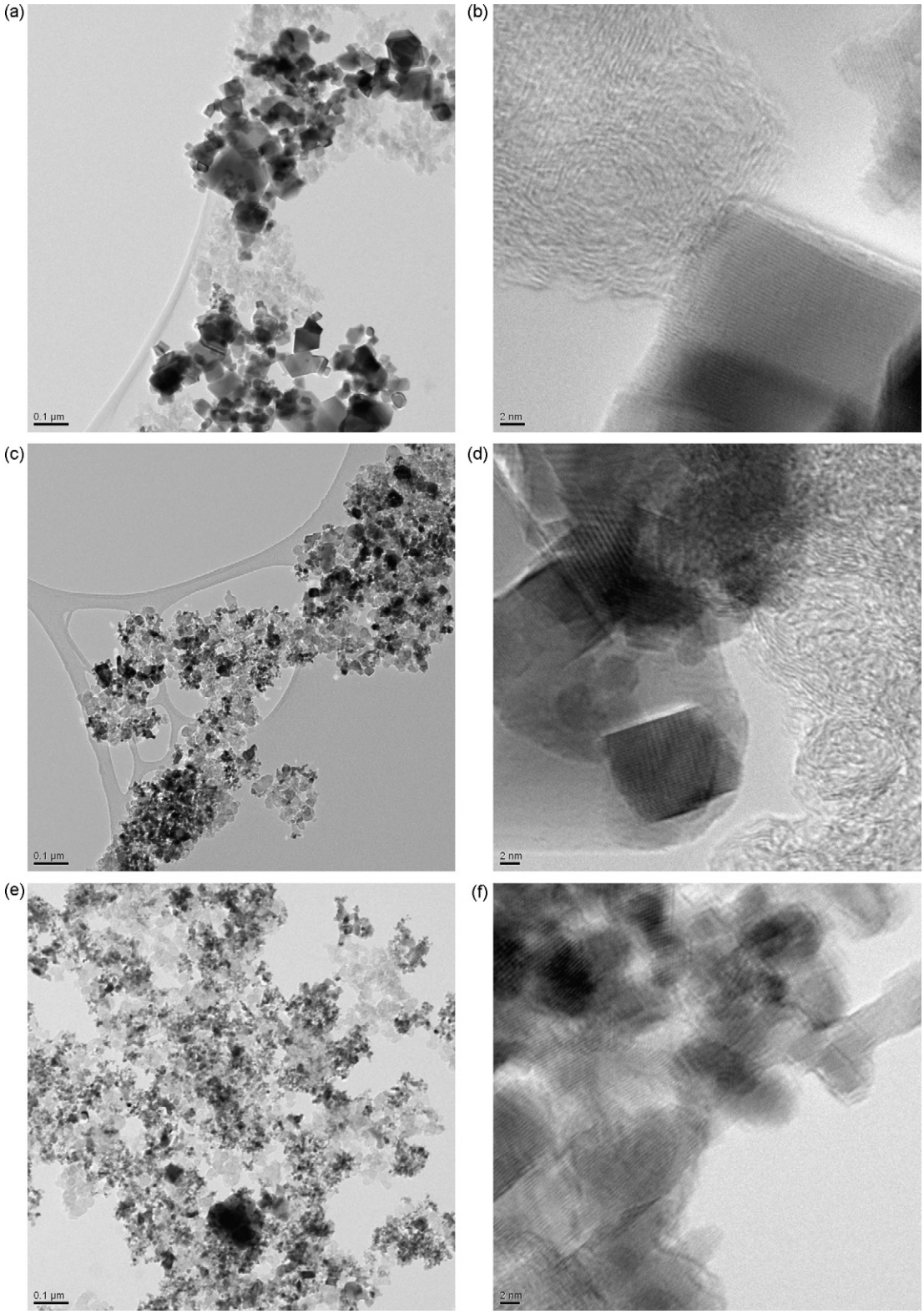

Fig. 6. Transmission electron microscopy (TEM) images of soot-catalyst mixtures prepared by the wet contact method. a) Overview AdNanoCeria with S_{BET} = 22 m^2/g; b) "feathery" contact between VP AdNanoCeria 50 with S_{BET} = 22 m^2/g cubic crystals and soot; c) overview VP AdNanoCeria 50 with S_{BET} = 60 m^2/g; d) detail of contact between VP AdNanoCeria 50 with S_{BET} = 60 m^2/g and soot; e) overview VP AdNanoCeria 50 with S_{BET} = 90 m^2/g; f) detail of "deep" contact between VP AdNanoCeria 50 with S_{BET} = 90 m^2/g and soot.

est T_{50} values. These measurements demonstrate that this order of combustibility is independent from the contact mode (see Fig. 3).

But as shown in Fig. 4, the soot combustion temperatures in their absolute form are strongly dependent on the contact mode. For the three classic contact modes exists a fixed order concerning the T_{50} value: tight < loose < pressure. The new created wet contact has not a fixed position within this order. While with PU soot on VP AdNanoCeria 50 the wet contact is between the tight and the loose contact, with P90 and FS the T_{50} value is even lower than in case of the tight contact. In view of the standard deviations of the characteristic temperatures all in all wet and tight contact show similar T_{50} values, but the former being more reproducible.

3.3. Double peak structure evaluations

Another interesting point of the new wet contact is the appearance of a double peak structure with the P90 soot in the DSC curve with varying peak areas depending on the surface area of ceria. With the standard VP AdNano Ceria 50 (with $S_{BET} = 60\,m^2/g$) two peaks, having a similar peak area, can be observed (see Fig. 5a). If the surface area decreases to $S_{BET} = 22\,m^2/g$ (Fig. 5b) the first peak nearly disappears, while the second peak increases. On the contrary a surface area of $S_{BET} = 90\,m^2/g$ causes a peak area decrease of the second peak and an increase of the first peak (as shown in Fig. 5c). Such behaviour is also indicated for the two other contact types, loose and tight contact mode, in the thermogravimetric curves as seen for instance in Fig. 3b: this means that differentiation in contact is latently present in all contact types, but the wet contact amplifies these differences significantly.

This observation can easily be explained by TEM images. In the case of a $S_{BET} = 22\,m^2/g$ surface area, large areas with agglomerated soot particles can be detected, while there is little direct contact of the catalyst particles with the soot (Fig. 6a). Fig. 6b shows the very "feathery" contact between ceria and soot. On the contrary VP AdNanoCeria 50 with $S_{BET} = 60\,m^2/g$ shows less areas of soot-soot interaction (Fig. 6c), while the amount of soot with a direct contact to the ceria catalyst increases. This intimate intermixture of soot and ceria shows that the contact between soot and VP AdNanoCeria 50 is better (Fig. 6d). With the VP AdNanoCeria 50 ($S_{BET} = 90\,m^2/g$), almost no areas of purely soot-soot interaction can be detected (Fig. 6e), because most of the soot is in the "deep" contact mode (Fig. 6f). Thus the soot combusts at very low temperatures. Especially in the pressure contact such a separation of interactions occurs too, explaining that despite the higher pressure compared to the tight contact the combustion temperatures of the pressure contact are often higher than those of the tight contact. Due to the high pressure applied the soot particles agglomerate, because the interaction forces are quite different to those of ionic compounds as ceria.

Comparing the TGA/DSC-curves and the TEM images, the double-peak structure can be explained if one assumes that the first peak describes the amount of soot, which is in the deep contact and the second peak describes the amount of soot, which is in the feathery or no contact.

3.4. Influence of the solvent on wet contact mode

To check, if there is any influence of the solvent on the characteristic temperatures and peak areas of the double peak structure, different solvents have been screened. VP AdNanoCeria 50 ($S_{BET} = 60\,m^2/g$) and P90 soot were used for these tests. After removal of the solvent by drying the samples were tested on soot combustion by TGA. In the temperature range up to 150 °C no significant differences of the thermogravimetric data compared to the tight and loose contact mode samples have been obtained indicating that the samples have been solvent free (see Fig. 4). The largest influence on the double peak areas had pentane and acetone, the smallest influence was detected in the case of water, where no mixture between soot and ceria was seen (see Table 4). Another interesting point of these different solvents is that also the T_{50} values of the wet contact strongly depend on the solvent used. Solvents creating a weak or no double peak structure reveal a T_{50} value, which is in the same range as that of the loose contact. Consequently, the wet contact has the additional advantage compared to tight and loose contact of being able to adjust the contact intensity simply by using different solvents. Also the stirring speed and time have effects on the combustion temperatures. As long as all these parameters are fixed during a series of experiments the results are highly reproducible.

Table 4
Influence of different solvents on the double peak effect of the wet contact mode.

Solvent	Double peak structure	T_{50} [°C]
Acetone	Strong	433
Pentane	Strong	496
Isopropanol	Middle	513
Hexane	Middle	519
Methanol	Middle	521
Ethanol	Middle	522
Isooctane	Middle	539
Toluene	Weak	540
Tetrahydrofuran	Weak	544
Benzene	Weak	550
Acetonitrile	Weak	552
Chloroform	No	569
Ethyl acetate	No	579
Water	No	588

4. Summary and outlook

The newly created wet contact mode has the advantage that it reveals a higher homogeneity and a higher reproducibility compared with the already established soot catalyst contact modes. This is not only very useful in the screening of different catalysts on activity in a high-throughput workflow, but represents an advantage *per se* with the additional benefit of offering the possibility for fine tuning by changing the solvent used and the stirring time. Additional advantages are the possibility of facile automation and the absence of influences due to operating personnel. The wet contact has the property that in TGA measurements a double peak, which depends on the surface area and the solvent, appears. This is achieved because within the wet contact different modes of contact can be further differentiated from TEM images, which we called "feathery" and "deep" contact to separate them from other contact modes as loose and tight contact. This different contact "arrangements" are also latently present in other contact types as loose or tight contact. With a well-selected solvent a T_{50} temperature can be reached, which is in the same range as that in real DPF systems. In future work the dependency of other influences will be investigated. We actually apply this new wet contact mode for the discovery and optimization of new soot combustion catalysts. In our HTE cycles a Chemspeed Accelerator SLT 106 with a solid dosing unit (SDU) is used for soot dosage as well as wet contact realization.

Acknowledgement

Funding of this project by the BMBF under the promotional reference FKZ 033R018G is gratefully acknowledged. We also thank Dr. M. Kröll from the Evonik-Degussa Corp. for supplying VP AdNanoCeria 50 with different surface areas and P90 soot as well as Dipl.-Ing. J. Schmauch from the Technical Physics Department of the Saarland University for the TEM measurements.

References

[1] J.P.A. Neeft, M. Makkee, J.A. Moulijn, Applied Catalysis B: Environmental 8 (1996) 57–78.
[2] J.F. Lamonier, N. Sergent, J. Matta, A. Aboukais, Journal of Thermal Analysis and Calorimetry 66 (2001) 645–658.
[3] B. Dernaika, D. Uner, Applied Catalysis B: Environmental 40 (2003) 219–229.
[4] A. Bueno-Lopez, K. Krishna, M. Makkee, J.A. Moulijn, Catalysis Letters 99 (2005) 203–205.
[5] A. Setiabudi, J. Chen, G. Mul, M. Makkee, J.A. Moulijn, Applied Catalysis B: Environmental 51 (2004) 9–19.
[6] E. Aneggi, C. de Leitenburg, G. Dolcetti, A. Trovarelli, Catalysis Today 114 (2006) 40–47.
[7] E. Aneggi, M. Boaro, C. de Leitenburg, G. Dolcetti, A. Trovarelli, Catalysis Today 112 (2006) 94–98.
[8] E. Aneggi, M. Boaro, C. de Leitenburg, G. Dolcetti, A. Trovarelli, Journal of Alloys and Compounds 408–412 (2006) 1096–1102.
[9] K. Krishna, A. Bueno-Lopez, M. Makkee, J.A. Moulijn, Topics in Catalysis 42/43 (2007) 221–228.
[10] K. Krishna, A. Bueno-Lopez, M. Makkee, J.A. Moulijn, Applied Catalysis B: Environmental 75 (2007) 210–220.
[11] K. Krishna, A. Bueno-Lopez, M. Makkee, J.A. Moulijn, Applied Catalysis B: Environmental 75 (2007) 201–209.
[12] K. Krishna, A. Bueno-Lopez, M. Makkee, J.A. Moulijn, Applied Catalysis B: Environmental 75 (2007) 189–200.
[13] M.A. Malecka, L. Kepinski, W. Mista, Applied Catalysis B: Environmental 74 (2007) 290–298.
[14] I. Atribak, I. Such-Basanez, A. Bueno-Lopez, A. Garcia, Journal of Catalysis 250 (2007) 75–84.
[15] P. Palmisano, N. Russo, D. Fino, C. Badini, AIChE Annual Meeting Conference Proceedings, San Francisco, CA, United States, Nov.12–17, 2006 (399d-1-399d/14).
[16] P. Palmisano, N. Russo, P. Fino, D. Fino, C. Badini, Applied Catalysis B: Environmental 69 (2006) 85–92.
[17] S.B. Simonsen, S. Dahl, E. Johnson, S. Helveg, Journal of Catalysis 255 (2008) 1–5.
[18] M. Machida, Y. Murata, K. Kishikawa, D. Zhang, K. Ikeue, Chemistry of Materials 20 (2008) 4489–4494.
[19] E.E. Iojoiu, B. Bassou, N. Guilhaume, D. Farrusseng, A. Desmartin-Chomel, K. Lombaert, D. Bianchi, C. Mirodatos, Catalysis Today 137 (2008) 103–109.
[20] Topas V2.1: General profile and structure analysis software for powder diffraction data, Bruker AXS, Karlsruhe, Germany, 1999.
[21] R.W. Cheary, A.A. Coelho, Journal of Applied Crystallography 25 (1992) 109–121.
[22] D. Fino, N. Russo, C. Badini, G. Saracco, V. Specchia, AIChE Journal 49 (2003) 2173–2180.
[23] D.S. Su, J.O. Müller, R.E. Jentoft, D. Rothe, E. Jacob, R. Schlögl, Topics in Catalysis 30/31 (2004) 241–245.
[24] EP 0 367 280 B2.
[25] H.J. Haepp, Physik in unserer Zeit 18 (1987) 162–168.
[26] N.E. Olong, K. Stöwe, W.F. Maier, Applied Catalysis B: Environmental 74 (2007) 19–25.
[27] S. Kureti, W. Weisweiler, K. Hizbullah, Applied Catalysis B: Environmental 43 (2003) 281–291.
[28] J.P.A. Neeft, O.P. van Pruissen, M. Makkee, J.A. Moulijn, Applied Catalysis B: Environmental 12 (1997) 21–31.